



HAL
open science

Concrete of tomorrow: corrosion performances in marine environment.

Elisabeth Marie Victoire, Véronique Bouteiller, Myriam Bouichou, Mirah Rakarabo, Victor da Silva, Amandine Bonnet, Lucas Adelaide, Philippe Turcry, Pauline Barthelemy, Jonathan Mai-Nhu, et al.

► **To cite this version:**

Elisabeth Marie Victoire, Véronique Bouteiller, Myriam Bouichou, Mirah Rakarabo, Victor da Silva, et al.. Concrete of tomorrow: corrosion performances in marine environment.. Concrete Solutions 2022 - the 8th International Conference on Concrete Repair, Durability and Concrete Technology, Jul 2022, Leeds, United Kingdom. 7 p., photos, graph., bibliogr. hal-04018305

HAL Id: hal-04018305

<https://hal.science/hal-04018305>

Submitted on 7 Mar 2023

HAL is a multi-disciplinary open access archive for the deposit and dissemination of scientific research documents, whether they are published or not. The documents may come from teaching and research institutions in France or abroad, or from public or private research centers.

L'archive ouverte pluridisciplinaire **HAL**, est destinée au dépôt et à la diffusion de documents scientifiques de niveau recherche, publiés ou non, émanant des établissements d'enseignement et de recherche français ou étrangers, des laboratoires publics ou privés.

Concrete of tomorrow: corrosion performances in marine environment

Elisabeth Marie-Victoire^{1,2*}, Véronique Bouteiller³, Myriam Bouichou^{1,2}, Mirah Rakarabo^{1,2}, Victor Da-Silva³, Amandine Bonnet³, Lucas Adelaïde³, Philippe Turcry⁴, Pauline Barthelemy⁵, Jonathan Mai-Nhu⁵, François Cussigh⁶

¹Laboratoire de Recherche des Monuments Historiques (LRMH), Ministère de la Culture, 29 rue de Paris, 77420 Champs-sur-Marne, France

²Sorbonne Universités, Centre de Recherche sur la Conservation (CRC, UAR 3224), Museum national d'Histoire naturelle, Ministère de la Culture, CNRS; CP21, 36 rue Geoffroy-Saint-Hilaire, 75005 Paris, France

³Univ Gustave Eiffel, MAST-EMGCU, F-77454 Marne - la- Vallée, France

⁴Laboratoire des Sciences de l'Ingénieur pour l'Environnement, UMR 7356 CNRS, La Rochelle Université, La Rochelle, France

⁵CERIB, 1 rue des longs Réages - CS 10010 - 28233 Epernon cedex, France

⁶Vinci Construction France, Nanterre, France

Abstract. Concrete is the most construction material used worldwide, but it often faces durability issues due to rebar corrosion, and cement production can be energy consuming. Attempts to improve its resilience versus corrosion while reducing its carbon footprint are ongoing at an international level. In this objective, in France within the frame of the national project PERFDUB, a series of reinforced concrete walls were cast with innovative concrete design, two shapes of rebars and two concrete covers. The standard performances of the different concrete mix designs were evaluated at a laboratory scale. Then the walls were exposed in the French La Rochelle harbor, in tidal zone in order to monitor the evolution of the corrosion of the bars for a period of twenty years. The first results of the electrochemical follow-up of these reinforced walls are presented in this paper.

1 Introduction

Within the frame of the French national project PERDUB [1], an intensive series of studies mixing lab scale, natural ageing and durability modelling was launched in 2015. The aims of the project are multiple. One of these is to provide innovative concrete mix designs to improve durability performances and lower carbon footprint. Another one is to characterize the performances of these concretes, especially against carbonation and chloride ingress. For the latest, a vast database of performances is being produced at the lab scale in combination with life cycle modelling. A last part of the project is dedicated to the evaluation of the performances of 11 of the concrete mixes designed against corrosion induced by natural carbonation or exposure to marine environment, for a period of 20 years. To follow up the initiation and propagation phases of corrosion, an approach combining non-destructive testing, embedded sensors and corrosion modelling was adopted. In the present paper, the experimental program and the first non-destructive electrochemical tests performed on 11 walls exposed for a little more than a year to natural ageing on marine environment, in the harbor of La Rochelle (French Atlantic ocean shore) in tidal zone are presented.

2 Experimental program

2.1 Specimen

A series of 11 walls T-shaped, 0.16m-large, with two 1m² faces (1mx1m), and a foot (0.4x0.15m) to ensure their stability against the tide were cast (Fig. 1a).

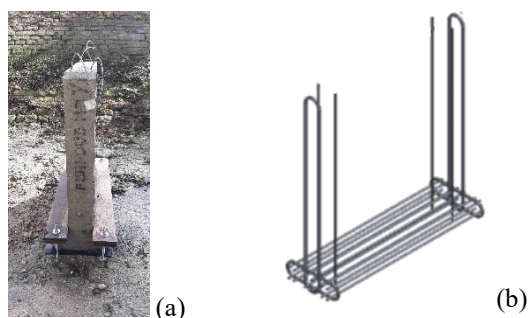


Fig. 1. a) Reinforced concrete wall specimens, b) Rebar network.

Two types of steel bars were embedded: smooth round shaped (RL) representative of ancient constructions

* Corresponding author: elisabeth.marie-victoire@culture.gouv.fr

(and which surface can be determined accurately for electrochemical calculations) and high-bond ribbed (HA) representative of modern ones. These rebars are isolated which means not in electrical contact with the others in the specimen. Two concrete covers were considered: 10mm and 20mm, to evaluate the progression of aggressive agents. Additional bars were added on the sides and foot of the walls for stability issues (Fig. 1b).

Eleven concrete mix designs with different binders were selected, from standard CEM I to binders containing mineral additions such as fly ashes (V), limestone filler (L), slag (S), silica fumes (FS), siliceous addition (AS), or metakaolin (MK). Due to these additions, the content of clinker was quite diverse with values ranging between 101 and 346 kg/m³ (Table 2). Different types of aggregates were chosen: two types of alluvial silico-limestones, one soft limestone and one hard limestone.

For each concrete mix design, water to binder ratios varying from 0.35 to 0.6 were considered (Table 2).

Compressive strengths measured on 3 cylinders of the same concrete after 28 days of wet curing (stored in water) were ranging between 29 and 103 MPa, while open porosities measured after 90 days of wet curing were varying between 10 and 20% (Table 3).

Table 1. Concrete binders and aggregates.

Concrete	Binder (kg/m ³)	Aggregates	
		Type	Water absorption (%)
B01	CEM I (289)	2	2.7
B02	CEM I (231) + fly ash (98)	2	2.7
B04	CEM III A (287)	2	2.7
B05	CEM I (122) + Slag (184)	2	2.7
B07	CEM I (267) + Limestone addition (188)	2	2.7
B31	CEM III A (383)	1	1.0
B36	CEM V (363)	4	4.0
B37	CEM V (374)	3	0.6
B38	CEM I (354) + Silica fume (30)	1	1.0
B40	CEM I (261) + siliceous addition (112)	2	2.7
B41	CEM I (302) + metakaolin (76)	1	1.0

Type 1 aggregate: Silica-limestone Alluvial, mixed rounded-crushed.

Type 2 aggregate: Silica-limestone Alluvial, round + mixed.

Type 3 aggregate: Dense limestone, crushed.

Type 4 aggregate: Limestone, crushed.

Table 2. Clinker content, water to binder ratio and water to cement ratio.

Concrete	Clinker content (kg/m ³)	W/B	W/C
B01	272	0.60	0.60
B02	217	0.54	0.77
B04	101	0.61	0.61
B05	115	0.57	1.44
B07	262	0.41	0.71
B31	137	0.4	0.4
B36	207	0.46	0.46
B37	207	0.45	0.45
B38	346	0.35	0.38
B40	245	0.47	0.67
B41	293	0.35	0.44

Table 3. Concrete preliminary laboratory characterization.

Concrete	Open porosity after 90 days of wet curing (%)	Compressive strength after 28 days of wet curing (MPa)	Chloride migration coefficient after 90±5 days of wet curing (x10 ⁻¹² m ² /s)
B01	16.9	28.8	19*
B02	17.4	31.9	5.7*
B04	16.7	49.9	2.5**
B05	18.6	44.5	2.0
B07	16.8	42.6	38
B31	12.1	61.6	0.4*
B36	19.6	49.9	11.7
B37	12.8	74.4	0.4
B38	10.3	103.5	0.2
B40	16.6	39.9	24.8
B41	10,8	88.5	0,8

*/** Test performed after 145±5 days (*) or 130 days (**) of wet curing

2.2 Monitoring

2.2.1 Measuring techniques

The first aim of the monitoring implemented in this study is to detect the corrosion initiation and afterwards to evaluate the corrosion activity in the propagation phase. The second one is to improve the accuracy of the corrosion diagnosis. Standard corrosion diagnosis is based on instant non-destructive electrochemical

measurements. However, previous studies have shown the impact of environmental conditions and specially rain events on the data collected, evidencing the need for continuous monitoring [2] [3] [4]. Nevertheless, those monitoring techniques have rarely been installed on real structures in natural ageing conditions [5] and still need to be validated. Therefore, the two types of technologies were considered and compared: embedded sensors and non-destructive testing.

Concerning the embedded sensors, for economic reasons, only three concretes B01, B04 and B31 were instrumented, and three additional walls were specifically cast. On those three walls, a complementary rebars network was introduced for the non-destructive measurements, and a series of sensors was embedded to monitor versus time: resistivity (Multi Ring Electrodes®); potential (ERE 20®); resistance, potential and corrosion current (Anode Ladder®). In a dedicated reservation, additional temperature and relative humidity sensors (HMP110®) were introduced from outside. Finally, all the sensors were connected to a multiplexer, itself connected to an analyzer, wired linked to a computer to provide data gathered in an automatic database [6]. Most of the sensors can deliver data at different depths allowing following the gradual ingress of aggressive agents into the concrete.

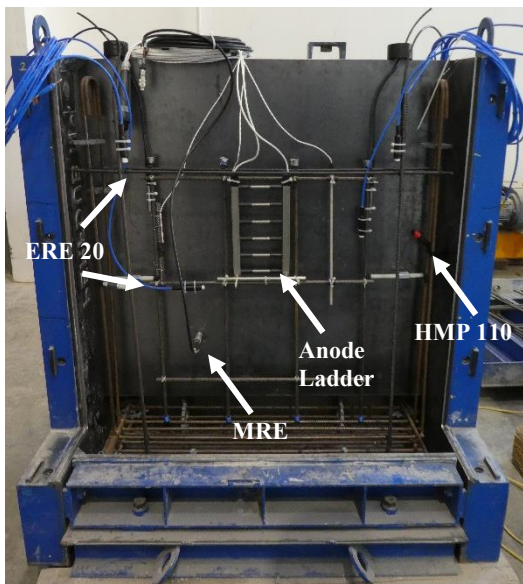


Fig. 2. Walls formwork and embedded sensors.

For the non-destructive testing, two types of techniques were considered: electrochemical tools [7] and evanescent field dielectrometry [8] [9]. Resistivity was measured with a four-point Wenner probe (Resipod®) [10] and with the disc method (Gecor10®) [11], potential mappings were performed with a copper/copper sulphate electrode (Canin®) [12] and corrosion rate was evaluated using a Gecor10® [13]

Only the first series of non-destructive electrochemical measurements on the eleven non-instrumented walls are presented in this paper.

2.2.2 Experimental protocol

The reinforced concrete walls were cast from December 2019 to January 2020. After almost one year of exposure to natural ageing in semi-rural environment, 60km south-west from Paris, they were implanted in December 2020 in marine environment in the harbor of La Rochelle.

The specimen are exposed to natural ageing in tidal zone (Fig.3a), which means around 6 hours immersed and 6 hours in the open air for every tide. As a consequence, the measurements can only be performed at low tide (Fig 3b) which means that to achieve the measurements on the eleven walls without embedded sensors (B01, B02, B04, B05, B07, B31, B36, B37, B38, BM40, B41), 10 days are necessary. The first set of experiments took place in October 2021.

The following protocol was adopted for the electrochemical measurements for each rebar (Fig.4) of each side of the walls (Fig. 5):

- Potential mapping [12], with 3 vertical lines spaced 5cm apart, with a measurement every 5cm,
- Resistivity measurements on point 8 (40cm from the top of the wall) and point 14 (70cm from the top of the wall), first with a 4-points (5cm spacing electrodes) Wenner probe (4 measurements per point according to the RILEM recommendation) [10] and second with the disc method (5 measurements per point 5cm spaced left and right from the rebar) [11],
- And one potential and LPR measurements on point 8 [13].

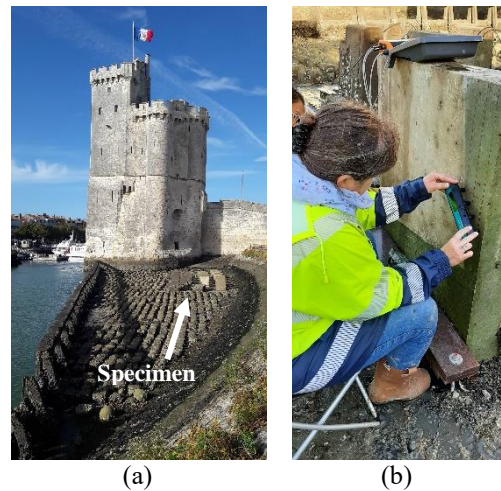


Fig. 3. a) Specimen in the tidal zone of La Rochelle harbor. b) Wenner resistivity measurement at low tide.

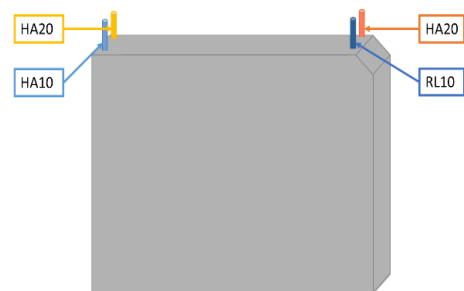


Fig. 4. For each type of rebar (RL and HA), two concrete covers were considered: 10mm and 20mm (RL10, RL20, HA10, HA20).

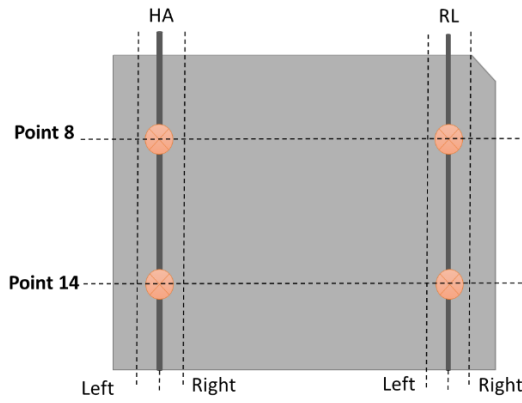


Fig. 5. On each face of the walls, potential mapping was performed on three vertical lines for each rebar (left, rebar, right), 4 points were considered for the resistivity measurements (point 8 and point 14 for each rebar) and LPR was only evaluated on point 8.

3 First results and discussions

3.1 Potential measurements

First, potential mapping clearly evidenced a difference between the two concrete covers, with less electronegative values of potential with the 20mm concrete cover (between -367 and -200mV, Fig. 6-8) than with 10 mm of concrete cover (between -560 and -317mV, Fig. 6-8). For example for wall B37, the shift is averagely varying from 100 to 200 mV between the two concrete covers (Fig.6). This could be linked to the moisture and salt contents, which are probably higher at lower depth.

Distinct results are also noted between the two rebars shapes, for both concrete covers, but no real trend emerges.

Another phenomenon can be observed on the potential maps, which exhibit an electronegative gradient from the top to the bottom of the walls on both faces, but clearer with the lowest concrete cover (RL10 and HA10, Fig. 6). The explanation could come from the duration of the tide's descent on the one hand, as the bottom of the walls stays wet a longer time (Fig. 8). On the other hand, when the tidal coefficient is low, the walls are not totally immersed (Fig. 9), which means that the top of the walls remains in the open air and can dry, while the bottom is totally under water.

When comparing the results of the 11 walls, B04, B36 and B40 exhibit the most electronegative values, while B31, B38, B41 lead to the less electronegative ones. For B04, the explanation could come from its W/B, and its high carbonation potential as the concrete is composed of a CEM III with low clinker content (Table 2). So that it is possible that the carbonation has progressed towards the lowest concrete cover of 10mm during the one year of exposure to natural ageing in semi-rural environment, before being implanted in marine environment. This carbonation could have favored the chlorides penetration, For B40, its quite high porosity and its high sensitivity to chloride migration (Table 3) may be the cause of these quite electronegative values. The same observation can be

done for B01 and B07, which exhibit quite electronegative values. Finally, for wall B36, its behavior is probably linked to its porous limestone as aggregates, its very high open porosity, and its quite high sensitivity to chloride penetration (Table 3).

RL10				MIN -531 MAX -317				HA10				MIN -560 MAX -327			
Point	Left	Rebar	Right	Point	Left	Rebar	Right	Point	Left	Rebar	Right	Point	Left	Rebar	Right
1	-340	-327	-325	1	-328	-328	-336	1	-328	-328	-336	1	-328	-328	-336
2	-339	-323	-324	2	-327	-330	-340	2	-327	-330	-340	2	-327	-330	-340
3	-335	-317	-320	3	-330	-330	-339	3	-330	-330	-339	3	-330	-330	-339
4	-339	-330	-326	4	-340	-341	-348	4	-340	-341	-348	4	-340	-341	-348
5	-342	-336	-331	5	-353	-353	-357	5	-353	-353	-357	5	-353	-353	-357
6	-350	-341	-336	6	-359	-358	-363	6	-359	-358	-363	6	-359	-358	-363
7	-358	-347	-341	7	-372	-370	-371	7	-372	-370	-371	7	-372	-370	-371
8	-367	-356	-357	8	-382	-381	-380	8	-382	-381	-380	8	-382	-381	-380
9	-381	-370	-364	9	-393	-393	-393	9	-393	-393	-393	9	-393	-393	-393
10	-395	-383	-380	10	-409	-408	-409	10	-409	-408	-409	10	-409	-408	-409
11	-410	-402	-398	11	-422	-417	-419	11	-422	-417	-419	11	-422	-417	-419
12	-428	-421	-415	12	-438	-434	-433	12	-438	-434	-433	12	-438	-434	-433
13	-442	-440	-437	13	-449	-441	-447	13	-449	-441	-447	13	-449	-441	-447
14	-462	-462	-454	14	-463	-457	-462	14	-463	-457	-462	14	-463	-457	-462
15	-488	-500	-481	15	-479	-475	-478	15	-479	-475	-478	15	-479	-475	-478
16	-500	-531	-502	16	-505	-512	-494	16	-505	-512	-494	16	-505	-512	-494
17	-504	-523	-508	17	-525	-535	-523	17	-525	-535	-523	17	-525	-535	-523
18	-506	-520	-509	18	-537	-550	-537	18	-537	-550	-537	18	-537	-550	-537
19	-497	-512	-498	19	-539	-560	-543	19	-539	-560	-543	19	-539	-560	-543

Fig. 6. Potential mapping on the face with a 10mm concrete cover.

RL20				MIN -367 MAX -245				HA20				MIN -377 MAX -200			
Point	Left	Rebar	Right	Point	Left	Rebar	Right	Point	Left	Rebar	Right	Point	Left	Rebar	Right
1	-245	-248	-256	1	-205	-205	-200	1	-205	-205	-200	1	-205	-205	-200
2	-260	-247	-253	2	-216	-209	-205	2	-216	-209	-205	2	-216	-209	-205
3	-257	-251	-252	3	-220	-207	-212	3	-220	-207	-212	3	-220	-207	-212
4	-260	-253	-252	4	-221	-210	-206	4	-221	-210	-206	4	-221	-210	-206
5	-262	-256	-251	5	-227	-226	-214	5	-227	-226	-214	5	-227	-226	-214
6	-262	-257	-248	6	-238	-227	-220	6	-238	-227	-220	6	-238	-227	-220
7	-270	-269	-260	7	-245	-239	-229	7	-245	-239	-229	7	-245	-239	-229
8	-278	-278	-277	8	-255	-245	-238	8	-255	-245	-238	8	-255	-245	-238
9	-288	-284	-272	9	-261	-248	-244	9	-261	-248	-244	9	-261	-248	-244
10	-298	-295	-289	10	-268	-259	-255	10	-268	-259	-255	10	-268	-259	-255
11	-305	-301	-285	11	-278	-271	-264	11	-278	-271	-264	11	-278	-271	-264
12	-315	-311	-312	12	-290	-279	-280	12	-290	-279	-280	12	-290	-279	-280
13	-323	-320	-320	13	-297	-293	-295	13	-297	-293	-295	13	-297	-293	-295
14	-339	-332	-324	14	-311	-311	-316	14	-311	-311	-316	14	-311	-311	-316
15	-350	-342	-339	15	-324	-328	-328	15	-324	-328	-328	15	-324	-328	-328
16	-358	-346	-343	16	-340	-338	-328	16	-340	-338	-328	16	-340	-338	-328
17	-365	-354	-353	17	-343	-343	-339	17	-343	-343	-339	17	-343	-343	-339
18	-365	-359	-353	18	-354	-348	-346	18	-354	-348	-346	18	-354	-348	-346
19	-367	-358	-359	19	-357	-347	-343	19	-357	-347	-343	19	-357	-347	-343

Fig. 7. Potential mapping on the face with a 20mm concrete cover.

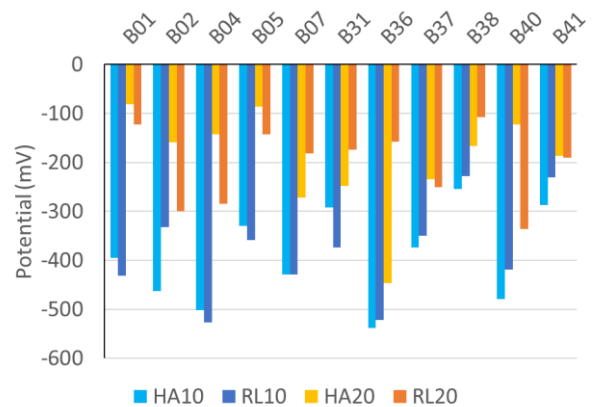


Fig. 8. Potential measured with the Gecor10® on point 8 of each rebar and concrete cover.



Fig. 9. During the tide's descent, the bottom of the walls remains a longer time immersed.



Fig. 10. At high tide of low coefficient, the top of the walls remains in the open air.

3.2 Resistivity measurements

Resistivity evaluated with the Wenner technique (Fig. 11) is consistent with the potential mapping, with the lowest values obtained for walls B40, B36 and B04. In addition, the walls B01 and B07 also exhibited quite low values, all indicative of corrosion favorable conditions, according to the RILEM recommendation. Contrarily, B31, B38, B41 showed the highest resistivity, which is also consistent with the potential mapping. As for the clear variations observed between the two concrete covers.

The results obtained with the Disc method (Fig. 12) are in line with that of the Wenner technique, but the measured values are generally lower (Fig. 13). This result has probably to do with the depth of concrete affected by the measurement, which is smaller for the Disc method than for the Wenner technique. Feliu et al. [11] demonstrated that at a depth equivalent to the disc diameter (2cm), the percentage of ohmic drop is already of 71%, reaching 81% at a depth of 3cm. As the Wenner probe used in this study had an electrode spacing of 5cm, the depth concerned by the measurement might be higher [14] than that of the Disc method. As it is probable that the concrete is wetter on the surface than in depth, this could explain why the resistivity measured with the 4-points method was generally higher than with the disc method.

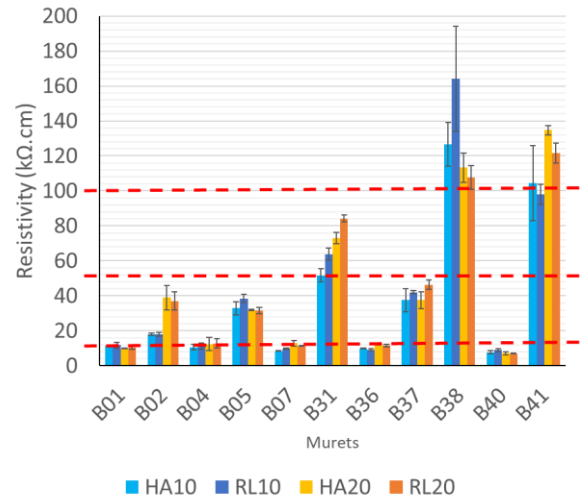


Fig. 11. Average resistivity value evaluated with the Wenner probe on point 8 and 14 for each rebar and concrete cover. RILEM thresholds in dashed lines.

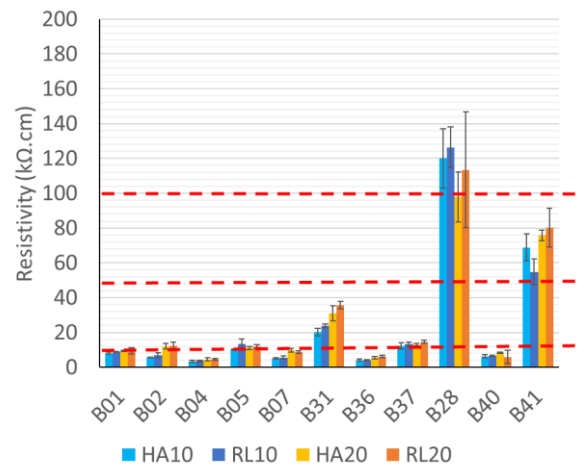


Fig. 12. Average resistivity evaluated with the Disc method probe on point 8 and 14 for each rebar and concrete cover. RILEM thresholds in dashed lines.

It has to be noted that with both techniques, slight differences can be observed between the two rebar shapes whatever the concrete cover. However, no trend emerges, as the variations are more or less in the range of the standard deviation for both measurement techniques.

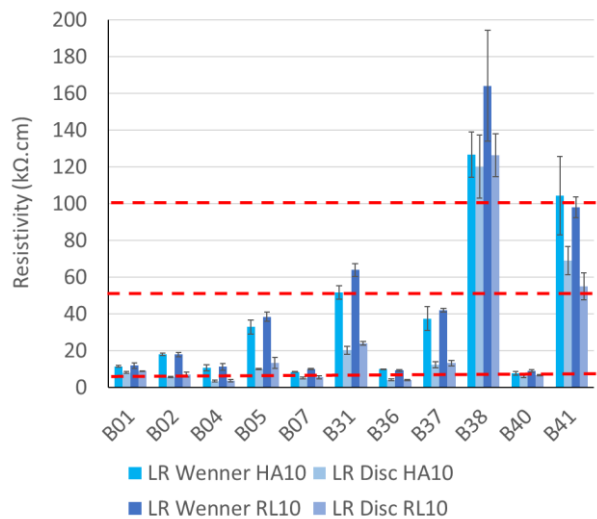


Fig. 13. Comparison (Wenner vs Disc) of the average resistivity evaluated on point 8 and 14 of each rebar with a 10mm concrete cover. RILEM thresholds in dashed lines.

3.3 Corrosion current density

The corrosion current densities are also consistent with the previous resistivity and potential measurements, with the highest values observed for designs B04, B36, B40 and B07 designs, and the lowest for B31, B38 and B41 (Fig. 14).

When referring to the RILEM recommendation [13] almost all the recorded values are above the first threshold of negligible corrosion ($0.1\mu\text{A}/\text{cm}^2$). Walls B04, B07, B36, B40, and punctually B02, lead to corrosion current densities higher than $0.5\mu\text{A}/\text{cm}^2$, which is the threshold of moderate corrosion. The threshold of $1\mu\text{A}/\text{cm}^2$ was exceeded only for the smallest concrete cover with designs B04 and B36. At this early stage of exposure to marine environment, except for the higher values (B04 and B36) the question of real rebars corrosion can be raised. Several hypothesis can be issued: is there enough oxygen at the rebars depth even at low tide? Is slag oxidation interfering with the rebars corrosion measurements? Is the pH of these new concrete designs high enough to protect the rebars? Are the existing RILEM threshold still adapted to the concretes containing mineral additions?

When comparing the values obtained with the two concrete covers, as for the preceding measurements, a tendency towards higher values for the lowest concrete cover is observed, for the same probable reasons.

Finally, has to be noted that for the highest concrete cover (20mm), the values are in the same range for both rebars shapes, except for walls B04 and B40. Contrarily, for the lowest concrete cover (10mm), generally higher values are observed for the high-bond shaped of rebars, except for B36. This might have to do with the calculation of the surface of rebar, which is more approximate for the high-bond shaped rebars.

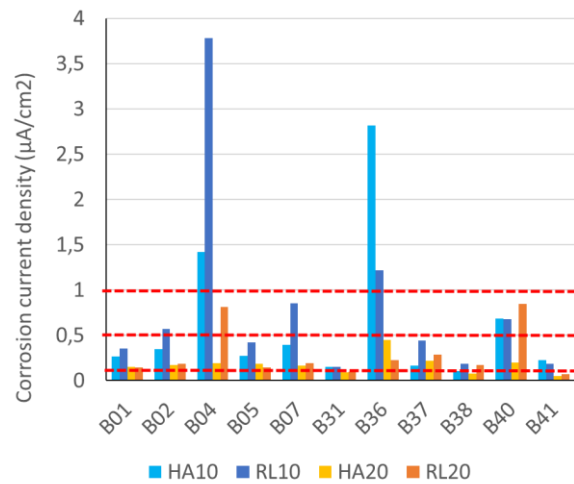


Fig. 14. Corrosion current density evaluated with a Gecor10[®] on point 8 for each rebar and concrete cover. RILEM thresholds in dashed lines.

4 Conclusions and outlooks

An intensive project PN-PERFDUB dedicated to the production and evaluation of several reinforced concrete, less polluting and more durable, was initiated in 2015 in France. Among the aims of the project, one is to produce a database on corrosion performances of 11 of the concretes in either conditions favorable for carbonation or marine environments, and a second one is to try to improve the accuracy of the corrosion diagnosis, by mixing instant non-destructive testing and permanent monitoring using sensors.

The first results of the non-destructive electrochemical measurements obtained after almost a year of natural ageing in marine environment showed noticeable differences between the concrete mix designs, but also a clear influence of the concrete cover and of the tide. Surprisingly due to the early stage of exposure, some of the concretes exhibited quite high corrosion current densities. At this step of the project, several questions can be raised: is the durability of some mix designs questionable? Is oxygen sufficiently available at low tide at the rebars depth? What is the influence of the mineral additions in the binders, especially the slag content? Are the RILEM threshold still adequate for concretes with high mineral additions content (limestone, metakaolin, slag...) which questions the adequacy of their pH value to protect the steel rebars?

The next phases of the project will help to clarify these points, as they include a comparison with embedded sensors and with complementary non-electrochemical non-destructive techniques (evanescent field dielectrometry). In addition, lab tests will be performed to evaluate, among a series of performances (open porosity, transfer coefficients, chlorides diffusion coefficients...), the chloride ingress and the carbonation depth. Therefore, sampling campaigns are scheduled in parallel to the non-destructive measurements and detailed observation of the law-walls, for the next 20 years. Finally, the data will be compared to that of the extensive laboratory tests

performed on these concretes in another part of the project, prior to the manufacture of the walls, and with the service life models.

The authors would like to thank the financial support of IREX and all the contributors of the PN-PERFDUB. They also would like to thank the City of La Rochelle, the La Rochelle Harbor, the Centre National des Monuments Nationaux, and the Yacht Club Classique for their logistical support and access authorization.

References

1. E. Rozière, A.Loukili, F. Cussigh: *A performance-based approach for durability of concrete exposed to carbonation*. In: Construction and Building Materials, Vol. 23 (2009) 1, pp.190-199
2. C. Andrade, A. Castillo: *Evolution of reinforcement corrosion due to climatic variations*, In: Materials and corrosion, Vol. 54, 2003, pp.379-386.
3. V. Bouteiller, J.-F. Cherrier, V. L'Hostis, N. Rebolledo, C. Andrade, E. Marie-Victoire, *Influence of humidity and temperature on the corrosion of reinforced concrete prisms*, In: European journal of environmental and civil engineering, vol. 16, n° 3-4, March-April 2012, pp. 471-480.
4. E. Marie-Victoire, V. Bouteiller, J. Montout, J.-L. Garciaz, E. Cailleux : *Parameters affecting on site corrosion rate evaluation*. In: Durable structures - from construction to rehabilitation, Proc. International conference, ICDS12, 31 May-1 June 2012, Lisbon, Portugal, 8p.
5. E. Marie-Victoire, M. Bouichou: *Corrosion at low moisture content in both carbonated and chloride polluted concrete – Villa E-1027, a case study*, In: Concrete solutions, Technical University of Cluj Napoca, Romania 30 Sept - 2 Oct 2019.
6. V. Bouteiller, G. Villain, B. Thauvin, E. Marie-Victoire, M. Bouichou : *Evaluation de la durabilité du béton armé vis-à-vis des ions chlorure à l'aide de capteurs noyés dans le béton versus des auscultations en parement*. In : Journées techniques GC 2019, Le génie civil au cœur des mutations technologiques et numériques, Cachan, France, 20-21th of March 2019
7. V. Bouteiller, L. Adelaïde, E. Marie-Victoire, M. Bouichou, B. Thauvin and G. Villain: *Non Destructive Testing and Corrosion Health Monitoring of reinforced concrete slabs submitted to chloride ions diffusion during five years*, In: Proceedings of the fib CACRCS DAYS 2021, Capacity Assessment of Corroded Reinforced Concrete Structures, on-line event, Edited by: Beatrice Belletti, Dario Coronelli, 30th November - 3rd December 2021
8. M. Bouichou, E. Marie-Victoire, H. Jourdan, B. Thauvin, R. Queguiner, R. Olmi, C. Riminesi : *Measurement of water content and salinity index in concrete by evanescent field dielectrometry*, In : Journal of Cultural Heritage, Vol. 34 (2018), pp. 237-246
9. E. Marie-Victoire, M. Bouichou, R. Olmi, C. Riminesi, V. Bouteiller: *On site electrochemistry vs. Evanescent Field Dielectrometry*, In: 12th ECNDT, Goteborg, Sweeden, 11-15th of June 2018, 8p.
10. R. Polder, C. Andrade, B. Elsener, O. Vennesland, J. Gulikers, R. Weidert, and M. Raupach: *Test methods for onsite measurement of resistivity of concrete, RILEM TC 154-EMC Recommendations*, IN: Materials and Structures, Vol. 33 (2000) pp.303-611.
11. S. Feliu, C. Andrade, J.A. Gonzalez, C. Alonso: *A new method for In-situ measurement of electrical resistivity of reinforced concrete*, In: Materials and structures, Vol. 29, July 1996, pp. 362-365.
12. B. Elsener, C. Andrade, J. Gulikers, R. Polder and M. Raupach: *Half-cell potential measurements – Potential mapping on reinforced concrete structures*, In: Materials and Structures, Vol. 36 (2003) pp 461-471.
13. C. Andrade, C. Alonso, J. Gulikers, R. Polder, R. Cigna, O. Vennesland, M. Salta, A. Raharinaivo and B. Elsener: *Test methods for on-site corrosion rate measurement of steel reinforcement in concrete by means of the polarization resistance method*, In: Materials and Structures, Vol. 37 (2004) pp. 623-643.
14. R. Du Plooy, S. Palma Lopes, G. Villain, X. Dérobert : *Development of a multi-ring resistivity cell and multi-electrode resistivity probe for investigation of cover concrete condition*, In: NDT&E International 54 (2013), pp.27-36.